

Syntheses and Structures of Cationic Bis(gold) Cyclopentadienyl Complexes

Brady L. Slinger, Jack C. Malek, and Ross A. Widenhoefer*

Department of Chemistry, Duke University, Durham, North Carolina (USA) 27708.

ABSTRACT: Reaction of $(P)AuOTf$ [$P = P(t\text{-Bu})_2$ -*o*-biphenyl] with cyclopentadienyl lithium reagents C_5H_5Li , C_5H_4MeLi , and C_5HMe_4Li forms the corresponding gold η^1 -cyclopentadienyl complexes $(P)Au(\eta^1\text{-}C_5H_5)$ (**3a**), $(P)Au(\eta^1\text{-}C_5H_4Me)$ (**3b**), and $(P)Au(\eta^1\text{-}C_5HMe_4)$ (**3c**), respectively in >60% isolated yield. Treatment of complexes **3a** or **3b** with $(P)AuNTf_2$ forms the corresponding cationic bis(gold) cyclopentadienyl complexes *trans*- $\{[(P)Au]_2(\eta^1,\eta^1\text{-cyclopentadien-1,3-yl})\}^+ NTf_2^-$ (**4a**), and *trans*- $\{[(P)Au]_2(\eta^1,\eta^1\text{-methylcyclopentadien-1,3-yl})\}^+ NTf_2^-$ (**4b**), respectively, in near quantitative yield which were characterized in solution and by X-ray crystallography. Both **4a** and **4b** undergo migration of the gold atoms about the cyclopentadienyl ring, which is fast on the NMR time scale at -80°C . In the solid-state, the gold atoms of **4a** and **4b** are positioned on opposite faces of the cyclopentadienyl ring above and below the C1 and C3 carbon atoms. Reaction of **3c** with $(P)AuNTf_2$ similarly forms the cationic bis(gold) tetramethylcyclopentadienyl complex $\{[(P)Au]_2(C_5HMe_4)\}^+ NTf_2^-$ (**4c**) although the structure of this complex remains obscure. The binding affinity of mono(gold) complexes **3a**-**3c** toward exogenous $(P)Au^+$ exceeds that of the corresponding unmetallated cyclopentadienes by more than three orders of magnitude. Protodeauration of bis(gold) complexes **4** with acetic acid at -80°C is >1500 times slower than is protodeauration of the corresponding monogold complexes **3** under identical conditions.

INTRODUCTION

A distinguishing feature of gold (I) complexes bearing unsaturated hydrocarbyl ligands, e.g., aryl, vinyl, and alkynyl, is their tendency to bind an exogenous twelve electron gold fragment (LAu^+) to form stable cationic bis(gold) complexes.¹⁻¹¹ Bis(gold) aryl and alkenyl complexes typically comprise a *gem*-diaurated carbon atom stabilized by an aurophilic Au–Au bond.²⁻⁷ Within this binding motif, the electronic structure varies between the limiting structures of a three-center, two-electron Au–C–Au bond or as a pair of two-electron Au–C bonds adjacent to a carbenium ion (Figure 1).^{2,3,11} In comparison, cationic bis(gold) alkynyl and some bis(gold) alkenyl complexes adopt an η^1,η^2 -structure possessing discrete and often rapidly interconverting σ - and π -bound gold atoms.^{4,9} Regardless of structure, these cationic bis(gold) complexes are characterized by their markedly lower reactivity with respect to electrophilic deauration relative to the corresponding neutral mono(gold) hydrocarbyl complexes.^{2-5,9} Owing to the diminished reactivity of cationic bis(gold) complexes toward electrophiles combined with the potentially high association constants for their formation,¹¹ cationic bis(gold) complexes are often formed under catalytic conditions, typically as off-cycle catalyst reservoirs.^{5,10}

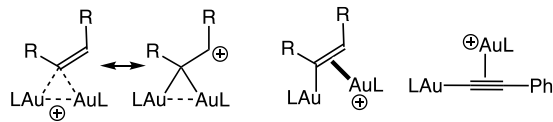
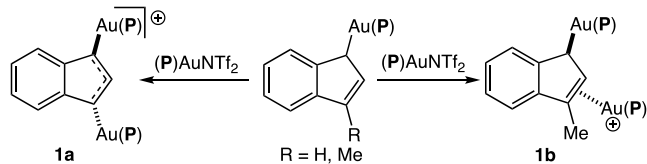


Figure 1. Binding modes of cationic bis(gold) complexes.

We have recently validated a new class of cationic bis(gold) complexes through the synthesis and characterization of cationic bis(gold) indenyl complexes **1a** and **1b** generated via the

reaction of the corresponding mono(gold) η^1 -indenyl complexes with $(P)AuNTf_2$ (Scheme 1).¹² The structures of bis(gold) indenyl complexes **1** are substitution dependent; the unsubstituted inden-1-yl complex **1a** adopts a \sim C2 symmetric *trans*-1,3- η^1,η^1 orientation, whereas the 3-methyl-inden-1-yl complex **1b** adopts a *trans*- η^1,η^2 orientation comprising isolated Au–C σ - and π -bonds (Scheme 1). The latter η^1,η^2 orientation has been documented for a number of transition metal μ -allyl complexes.¹³ Conversely, the *trans*-1,3- η^1,η^1 structure of **1a** has been previously observed only in the solid state for electrophilic In,¹⁴ Sc,¹⁵ Mn,¹⁶ and Ga¹⁷ cyclopentadienyl complexes with no evidence that these interactions persist in solution. Among the late transition metals, perhaps the closest analogs to complex **1a** are the dinuclear Ni and Pd μ -allyl, μ -indenyl, and μ -cyclopentadienyl complexes,^{18,19} which are nevertheless distinct from **1a** owing to the *cis* arrangement of metals, the presence of a M–M bond, and a shorter M–C_{int} bond owing to M → allyl π -back bonding contributions that are absent in **1a**.¹⁹



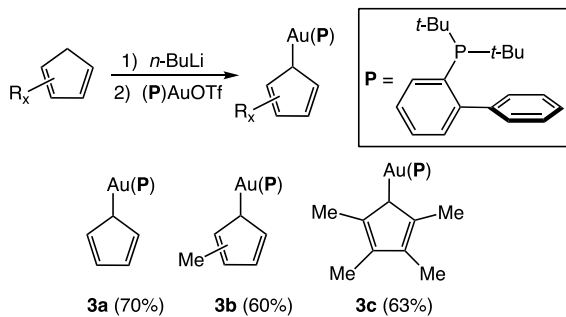
Scheme 1. Cationic bis(gold) indenyl complexes **1a** and **1b**.

Owing both to the potential relevance of cationic bis(gold) allyl complexes under catalytic conditions²¹ and the novel structure of **1a**, we sought to expand the scope of cationic bis(gold) allyl complexes beyond the indenyl framework. In doing so, we hoped to gain additional information regarding the factors that influence the structure and stability of these complexes.

Similarly, because assignment of the novel *trans*-1,3- η^1,η^1 structure of **1a** relied heavily on computation,¹² we sought to validate this unusual bonding arrangement experimentally via X-ray crystallography. Here we report that mononuclear gold η^1 -cyclopentadienyl complexes react with exogenous LAu⁺ to form the corresponding cationic bis(gold) cyclopentadienyl complexes. Single crystal X-ray analysis of bis(gold) cyclopentadienyl and methylcyclopentadienyl complexes established the *trans*-1,3- η^1,η^1 structure of these complexes.

RESULTS AND DISCUSSION

Synthesis of gold cyclopentadienyl complexes. Toward the objective of expanding the scope of cationic bis(gold) allyl complexes, gold cyclopentadienyl complexes emerged as attractive targets for investigation. In contrast to the dearth of simple aliphatic gold η^1 -allyl complexes,^{22,23} substituted and unsubstituted gold(I) cyclopentadienyl complexes containing a triphenylphosphine or trialkylphosphine ligand have been known for decades,^{24,25} although the less substituted C₅H₅ and C₅H₄Me complexes display limited thermal stability.²⁵ Guided by our investigation of gold indenyl complexes,¹² we reasoned that employment of the more sterically hindered P(*t*-Bu)₂*o*-biphenyl (**P**) supporting ligand might enhance the thermal stability of mono(gold) cyclopentadienyl complexes allowing for isolation and investigation. To this end, transmetalation of cyclopentadienyl-, methylcyclopentadienyl- or 2,3,4,5-tetramethylcyclopentadienyllithium with (**P**)AuOTf in THF at 25 °C led to isolation of the gold cyclopentadienyl complexes (**P**)Au(η^1 -C₅H₅) (**3a**), (**P**)Au(η^1 -C₅H₄Me) (**3b**), and (**P**)Au(η^1 -C₅HMe₄) (**3c**), respectively, in >60% yield as yellow-brown solids (Scheme 2). Complexes **3** were stable indefinitely under N₂ at 4° C in the solid state but decomposed within 12 h in solution at room temperature taking on a purple hue, suggesting the formation of colloidal gold(0),²⁶ with formation of free cyclopentadiene and cyclopentadienide.



Scheme 2. Synthesis of gold cyclopentadienyl complexes 3.

In accord with previous observations regarding gold cyclopentadienyl^{24,25} and transition metal η^1 -cyclopentadienyl complexes,²⁷ NMR spectroscopy of **3a** was consistent with rapid migration of gold about the cyclopentadienyl ring, presumably via successive [1,5] sigmatropic rearrangements.²⁸ For example, the ¹H NMR spectrum of **3a** at -80 °C displayed a five-proton singlet at δ 5.54 assigned to the cyclopentadienyl protons while the ¹³C NMR spectrum of **3a** at -80 °C displayed a single resonance at δ 109.6 (d, $J_{\text{CP}} = 7.0$ Hz) assigned to the cyclopentadienyl carbon atoms. In the solid state, **3a** adopts a distorted η^1 -cyclopentadien-1-yl structure with weak interactions between the gold atom and the C2 and C5 cyclopentadienyl carbon atoms (Figure 2), as has been documented for other gold cyclopentadienyl complexes.^{24,25} For example, the Au–C1–C2

(101°) and Au–C1–C5 (95.9°) bond angles are compressed relative to an idealized Au–C(sp³) bond. The Au–C1 (2.140 Å) bond distance is typical of a Au–C(sp³) bond,²⁹ with longer Au–C2 (2.807 Å) and Au–C5 (2.714 Å) distances. The structure of **3a** displays an interesting distortion away from Cs symmetry with the cyclopentadienyl ligand rotated toward one of the phosphorus-bound *t*-Bu groups with concomitant displacement of the protruding ortho phenyl group away from the cyclopentadiene ligand (Figure 2).

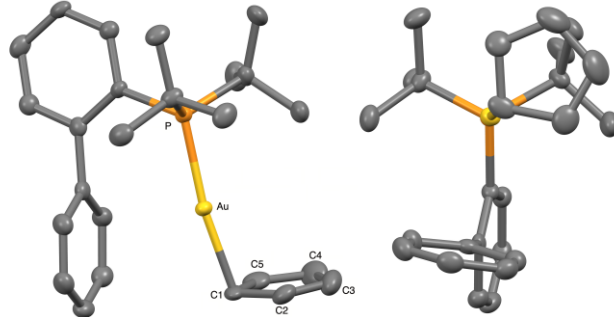
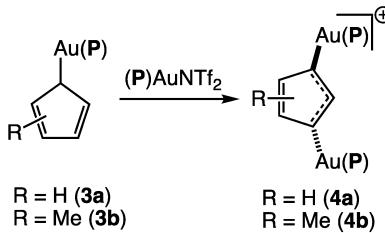


Figure 2. Ortep diagram of (**P**)Au(C₅H₅) (**3a**) with ellipsoids shown at 50% probability and with hydrogen atoms omitted for clarity (left). Identical structure viewed along the Au–P bond (right). Calculated bond lengths (Å) and bond angles (°): Au–P = 2.271(1), Au1–C1 = 2.140(5), Au–C2 = 2.807(4), Au–C5 = 2.714(6), C1–C2 = 1.442(5), C2–C3 = 1.353(7), C3–C4 = 1.433(7), C4–C5 = 1.366(6), C1–C5 = 1.463(6), P–Au–C1 = 171.9(1), Au–C1–C2 = 101.4(3), Au–C1–C5 = 95.9(3).

As was the case with **3a**, the spectroscopy of methylcyclopentadienyl complex **3b** was consistent with facile migration of gold about the methylcyclopentadienyl ligand. The ¹H NMR spectrum of **3b** at -80 °C displayed a three-proton singlet at δ 1.99 assigned to the cyclopentadienyl methyl group and a pair of two proton singlets at δ 5.22 and 5.04 assigned to the cyclopentadienyl CH protons. Similarly, the ¹³C NMR spectrum of **3b** at -80 °C displayed a singlet at δ 16.2 assigned to the cyclopentadienyl methyl group and two broad phosphorus-coupled doublets at δ 107.0 ($J_{\text{HP}} = 10.6$ Hz) and 109.0 ($J_{\text{HP}} = 9.1$ Hz) assigned to the two cyclopentadienyl CH carbon atoms. In contrast, the spectroscopy of tetramethylcyclopentadienyl complex **3c** was consistent with a static structure with gold bound to the cyclopentadienyl CH carbon atom. In particular, the ¹H NMR spectrum of **3c** at -80 °C displayed a phosphorus-coupled doublet at δ 2.12 ($J_{\text{HP}} = 14.8$ Hz) assigned to cyclopentadienyl CH proton. The ¹³C NMR spectrum of **3c** at -80 °C displayed a phosphorus-coupled doublet at δ 71.2 ($J_{\text{CP}} = 61.3$ Hz) assigned to the cyclopentadienyl CH carbon atom. Worth noting, this phosphorous-carbon coupling constant is much larger than is J_{CP} observed for the cyclopentadienyl CH carbon resonances of complexes **3a** and **3b**, even when considering the fluxionality of the latter structures. For example, the 7.0 Hz doublet observed for **3a** presumably reflects the time-averaged composite of one 35 Hz doublet and four singlets (i.e. $J_{\text{CP}} = 0$ Hz). The significantly larger phosphorous-carbon coupling constant observed for **3c** ($J_{\text{CP}} = 61.3$ Hz) presumably reflects the greater s-orbital character of the Au–C bond of **3c** relative to the Au–C bonds of **3a** and **3b**.

Synthesis of cationic bis(gold) cyclopentadienyl complexes. Reaction of an equimolar mixture of **3a** or **3b** with (**P**)AuNTf₂ in CH₂Cl₂ at 25 °C rapidly (≤ 1 min) and

quantitatively formed the corresponding cationic bis(gold) cyclopentadienyl complexes *trans*-{[(P)Au]₂(η^1 , η^1 -cyclopentadien-1,3-yl)}⁺ NTf₂⁻ (**4a**; NTf₂ = (CF₃SO₂)₂N], and *trans*-{[(P)Au]₂(η^1 , η^1 -methylcyclopentadien-1,3-yl)}⁺ NTf₂⁻ (**4b**), respectively (Scheme 3). Both **4a** and **4b** were isolated as yellow-brown crystals via slow diffusion of hexanes into concentrated CH₂Cl₂ solutions and were characterized by spectroscopy and by X-ray crystallography.



Scheme 3. Synthesis of cationic bis(gold) cyclopentadienyl complexes **4a and **4b**.**

In the solid state, **4a** adopts approximate C_2 symmetry about the cyclopentadiene ring with the gold atoms positioned on opposite faces of the cyclopentadienyl ring above and below the C1 and C3 carbon atoms (Figure 3). The Au1–C1 and Au2–C3 bond lengths of 2.180 Å are nominally longer the Au–C1 bond in monogold complex **3a** (2.140 Å). Both gold atoms of **4a** are displaced slightly toward the central C2 carbon atom with Au1–C1–C2 and Au2–C3–C2 angles of 90.9 and 89.3°, respectively, compared to Au1–C1–C5 and Au2–C3–C4 angles of 95.7 and 97.7°, respectively, and with Au1–C2 and Au2–C2 distances of 2.611 and 2.604 Å, respectively, compared to Au1–C5 and Au2–C4 distances of 2.73 and 2.754(6) Å, respectively. The ortho phenyl rings of the P(t-Bu)₂*o*-biphenyl ligands are directed toward the cyclopentadienyl ring with closest Au–C_{arene} contacts of 3.02 Å. Bonding within the cyclopentadienyl ligand, notably the shorter the C4–C5 bond (1.344 Å) and longer C3–C4 (1.451) and C1–C5 (1.442) bonds. points to distortion toward isolated allyl and alkenyl groups.

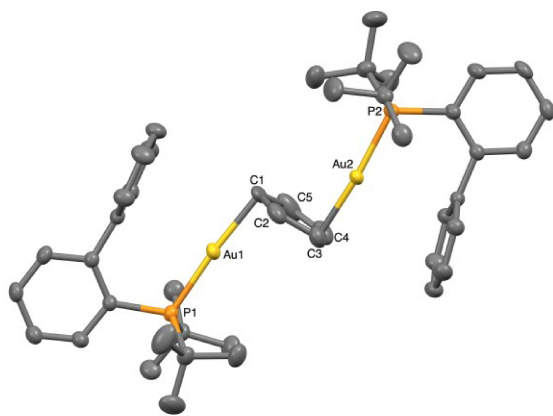


Figure 3. Ortep diagram of *trans*-{[(P)Au]₂(η^1 , η^1 -cyclopentadien-1,3-yl)}⁺ NTf₂⁻ (**4a**) with ellipsoids shown at 50% probability and with counterion and hydrogen atoms omitted for clarity. Calculated bond lengths (Å) and bond angles (°): Au1–C1 = 2.180(7), Au1–C2 = 2.611(7), Au1–C5 = 2.73(1), Au2–C3 = 2.180(7), Au2–C2 = 2.604(7), Au2–C4 = 2.754(6), C1–C2 = 1.405(8), C2–C3 = 1.416(8), C3–C4 = 1.451(7), C4–C5 = 1.344(9), C1–C5 = 1.442(9), P1–Au1–C1 = 174.2(2), P1–Au1–C2 = 147.8(1), P2–Au2–C3 = 173.6(2), P2–Au2–C2 = 141.9(1), Au1–C1–C2 = 90.9(4), Au1–C1–C5 = 95.7(4), Au2–C3–C2 = 89.3(4), Au2–C3–C4 = 97.7(4).

The Au–C bond lengths and bond angles of bis(gold) cyclopentadienyl complex **4a** are similar to the values determined computationally for bis(gold) indenyl complex **1a** (Au1–C1 distance of 2.204, Au1–C2 = 2.697, Au–C1–C2 = 93.3, Au–C1–C9 = 103.8), which suggests that similar Au–C bonding interactions are involved in both complexes. The Au-indenyl bonding of **1a** was interpreted as arising from overlap between the filled antisymmetric $2\pi_a$ and $1\pi_a$ indenyl molecular orbitals with the symmetric combination of the P–Au anti-bonding orbitals [$\phi_a(\sigma^*)$] (Figure 4). The cyclopentadienyl $2\pi_b$ molecular orbital is related to the indenyl $2\pi_a$ and $1\pi_a$ molecular orbitals, which contain in phase ($1\pi_a$) and out of phase ($2\pi_a$) contributions of the phenyl π system. Therefore, the primary gold-cyclopentadienyl bonding of **4a** presumably involves overlap between the filled antisymmetric cyclopentadienyl $2\pi_b$ molecular orbital with P–Au anti-bonding orbitals $\phi_a(\sigma^*)$ (Figure 4). The similarity of the metal-ligand bonding interactions for bridging indenyl and cyclopentadienyl ligands was likewise noted for dipalladium μ -cyclopentadienyl and μ -indenyl complexes.¹⁹

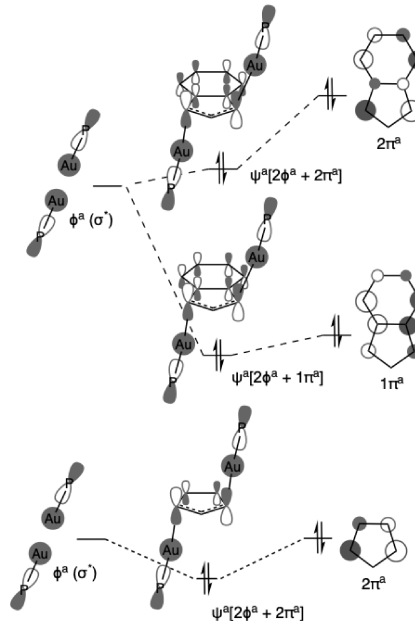
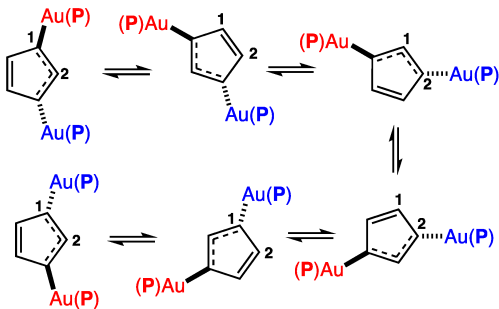


Figure 4. Orbital mixing diagrams describing the gold-indenyl bonding of **1a** (top) and (b) the gold cyclopentadienyl bonding of **4a** (bottom).

As was the case with the parent mono(gold) complex **3a**, the spectroscopy of **4a** is consistent with facile migration of the two gold atoms about the cyclopentadienyl ring. For example, the ¹H NMR spectrum of **4a** at –80 °C displayed a five-proton singlet at δ 5.43 assigned to the cyclopentadienyl protons and the ¹³C NMR spectrum of **4a** at –80 °C displayed a single resonance at δ 108.0 assigned to the cyclopentadienyl carbon atoms. Sequential [1,5] migration of the two (P)Au groups of **4a** is sufficient to interconvert all positions of the cyclopentadienyl ligand and the absence of broadening of the cyclopentadienyl resonances in the ¹H and ¹³C NMR spectra at –80 °C points to an extremely facile fluxional process (Scheme 4).



Scheme 4. Interconversion of the five cyclopentadienyl positions of **4a** via sequential [1,5]-sigmatropic rearrangements.

The X-ray crystal structure of **4b** was complicated by the positional disorder of the cyclopentadienyl methyl group and the associated rotational disorder of one methyl group on each of the phosphorus atoms, corresponding to two regioisomeric forms of **4b** in the solid state (Figure 5). In the minor isomer the cyclopentadienyl methyl group (C6') is bonded to the cyclopentadienyl C2 carbon atom (**4ba**; 37% occupancy), and in the major isomer the cyclopentadienyl methyl group (C6) is bonded to the cyclopentadienyl C5 carbon atom (**4bb**; 63% occupancy). Although this positional disorder precluded detailed analysis of the bond distances and angles within the cyclopentadienyl ring, the crystal structure of **4b** established a distorted *trans*-1,3- η^1,η^1 structure analogous to that of **4a** with the gold atoms positioned on opposite faces of the cyclopentadienyl ring above and below the C1 and C3 carbon atoms (Figure 5).

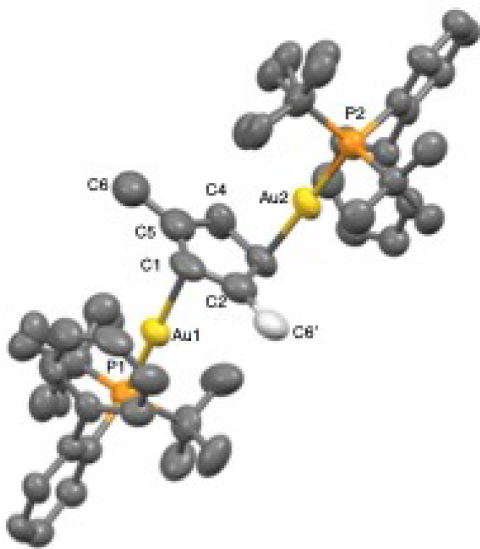


Figure 5. Ortep diagram of $\text{trans-}\{[(\text{P})\text{Au}]_2(1,3-\eta^1,\eta^1-\text{C}_5\text{H}_4\text{Me})\}^+\text{NTf}_2^-$ (**4b**) with ellipsoids shown at 50% probability and with counterion, hydrogen atoms, and minor occupancy P-Me groups omitted for clarity. Cyclopentadienyl methyl group C6 (dark gray, 63% occupancy) corresponds to major isomer **4bb**, while cyclopentadienyl methyl group C6' (light gray, 37% occupancy) corresponds to minor isomer **4ba**. Calculated bond lengths (\AA) and bond angles ($^\circ$): Au1–C1 = 2.19(2), Au1–C2 = 2.54(2), Au1–C5 = 2.74(3), Au2–C3 = 2.17(2), Au2–C2 = 2.71(2), Au2–C4 = 2.73(2), P1–Au1–C1 = 173.2(4), P2–Au2–C3 = 177.3(4), Au1–C1–C2 = 87(1), Au1–C1–C5 = 95(1), Au2–C3–C2 = 95(1), Au2–C3–C4 = 95(1).

Interestingly, the two gold atoms of **4b** are positioned unsymmetrically about the C1–C2–C3 unit with Au1 displaced toward C2 (Au1–C2 = 2.54 \AA) and Au2 displaced away from C2 (Au1–C2 = 2.71 \AA) relative to the more symmetric arrangement of the two gold atoms observed in **4a** (Au1/Au2–C2 = 2.611/2.604 \AA), suggesting a slight distortion of Au1 toward an η^2 bonding mode. We considered and ultimately rejected the possibility that minor isomer **4ba** adopts an η^1,η^2 bonding mode in the solid state owing to the stabilizing effect of the C2 methyl group on the C1=C2 bond with this contribution superimposed on the dominant η^1,η^1 -bonding of major isomer **4bb** in the disordered crystal (Figure 6). However, this possibility was rejected based on two observations. Firstly, we performed DFT analysis of $\text{trans-}\{1,3-\eta^1,\eta^1-[(\text{PMe}_3)\text{Au}]_2(2-\text{C}_5\text{H}_4\text{Me})\}^+$ ($\eta^1,\eta^1\text{-4ba}^*$) and $\text{trans-}\{\eta^1,\eta^2-[(\text{PMe}_3)\text{Au}]_2(2-\text{C}_5\text{H}_4\text{Me})\}^+$ ($\eta^1,\eta^2\text{-4ba}^*$) at the SMD(DCE)/TPSSh/aug-cc-pVTZ//B3LYP/6-31G(d) level of theory employing trimethylphosphine in place of $\text{P}(t\text{-Bu})_2$ -*o*-biphenyl (**P**) for computational simplicity (Figure 6). These calculations identified $\eta^1,\eta^1\text{-4ba}^*$ as the lower energy structure and indeed, $\eta^1,\eta^2\text{-4ba}^*$ did not represent a local minimum and collapsed to $\eta^1,\eta^1\text{-4ba}^*$ upon attempted minimization. Secondly, there is no evidence for disorder of the Au1 atom in the crystal structure of **4b**; the Au1 ellipsoids is of normal shape and the electron density maps reveal no additional positions in which a disordered Au atom could reside.

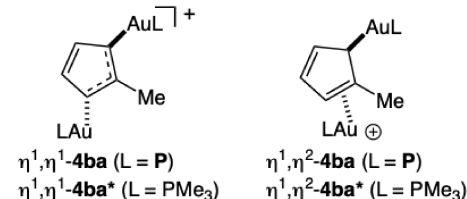
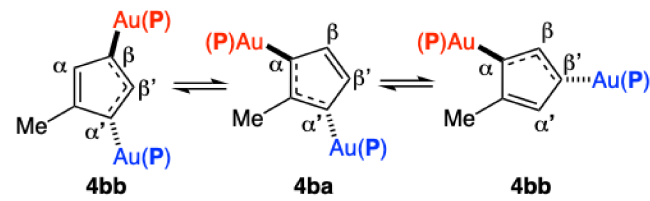


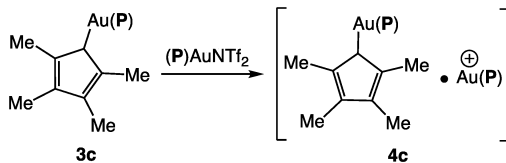
Figure 6. Structures of $\text{trans-1,3-}\eta^1,\eta^1\text{-}$ and $\text{trans-}\eta^1,\eta^2\text{-(LAu)}_2(\text{C}_5\text{H}_4\text{Me})^+$ ($\text{L} = \text{P, PMe}_3$) bearing a C2 cyclopentadienyl methyl group.

NMR spectroscopy established the static or time-averaged two-fold symmetry of **4b** in solution. For example, the ^1H NMR spectrum of **4b** at -80°C displayed a pair of two proton singlets at δ 5.13 and 4.80 assigned to the cyclopentadienyl protons, while the ^{13}C NMR spectrum a pair of closely spaced resonances at δ 103.5 and 103.7 assigned to the cyclopentadienyl CH carbon atoms and 11 additional $\text{C}(\text{sp}^2)$ carbon resonances (δ 125–149). These data are consistent either with the presence of a static **4ba** regioisomer or with a rapidly interconverting mixture of **4bb** isomers. Given the fluxional nature of cyclopentadienyl complex **4a**, this latter scenario appears more likely. Two sequential [1,5]-migrations are sufficient to interconvert the cyclopentadienyl methine groups and $(\text{P})\text{Au}$ groups of **4bb** via **4ba** (Scheme 5). The absence of broadening in the ^1H and ^{13}C NMR spectra of **4b** at -80°C points to a facile fluxional process.



Scheme 5. Interconversion of the potential isomers of **4b** via sequential [1,5]-sigmatropic rearrangements.

When an equimolar (~30 mM) mixture of the tetramethylcyclopentadienyl complex **3c** and $(\mathbf{P})\text{AuNTf}_2$ was dissolved in CD_2Cl_2 at room temperature, ^{31}P NMR analysis of the resulting solution at -80°C revealed formation of the corresponding cationic bis(gold) complex $\{[(\mathbf{P})\text{Au}]_2(\text{C}_5\text{HMe}_4)\}^+ \text{NTf}_2^-$ (**4c**) in >90% yield (Scheme 6). In contrast to bis(gold) complexes **4a** and **4b**, complex **4c** could not be isolated and was therefore characterized in solution without isolation. However, despite combined spectroscopic and computational analysis (see below), the structure of **4c** remains unclear. For example, the ^{13}C NMR spectrum of **4c** displays a pair of cyclopentadienyl methyl groups at δ 15.3 and 12.00 and 12 unique $\text{C}(\text{sp}^2)$ carbon resonances (δ 116–150). Particularly notable is a phosphorus-coupled triplet at δ 85.1 ($J_{\text{CP}} = 17$ Hz) in the ^{13}C NMR spectrum of **4c** assigned to the cyclopentadienyl CH carbon atom. Both this resonance and the cyclopentadienyl CH resonance at δ 3.18 in the ^1H NMR spectrum of **4c** are shifted to higher frequency and display diminished J_{CP} and J_{HP} values relative to the mono(gold) complex **3c** [$^{13}\text{C}[^1\text{H}]$ NMR: δ 71.19 (d, $J = 61.3$ Hz); ^1H NMR: δ 2.12 (d, $J = 14.8$ Hz)]. The ^{31}P NMR spectrum of **4c** displayed a single resonance at δ 60.4.



Scheme 6. Synthesis of cationic bis(gold) tetramethylcyclopentadienyl complex **4c**.

The NMR spectra of **4c** established the static or time-averaged two-fold symmetry of **4c** in solution, while the phosphorus-coupled triplet at δ 85.1 ($J_{\text{CP}} = 17$ Hz) in the ^{13}C NMR spectrum pointed to a structure with two $(\mathbf{P})\text{Au}$ groups bound to the CH cyclopentadienyl carbon atom. We initially considered two *gem*-diaurated structures consistent with this connectivity containing either a triangular (*cis,gem*-**4c**) or linear (*trans,gem*-**4c**) arrangement of the Au–C–Au atoms (Figure 7). Both structures are unusual; we are aware of no analog of *trans,gem*-**4c** and although *gem*-diaurated complexes are well known, the vast majority of these complexes contain a gold-bound $\text{C}(\text{sp}^3)$ atom as opposed to the *gem*-diaurated $\text{C}(\text{sp}^3)$ atom of complex *cis,gem*-**4c**.^{1–11} Rather, the closest analogs to structure *cis,gem*-**4c** are the cationic bis(gold) methyl complexes first reported by Campos.^{31,32}

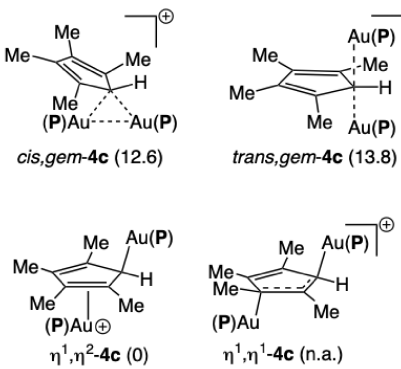
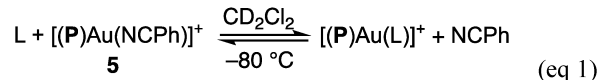


Figure 7. Optimized structures of potential isomers of $[(\mathbf{P})\text{Au}]_2(\text{C}_5\text{HMe}_4)^+$ (**4c**) with relative free energies in kcal/mol. The structure indicated as N/A was not located as a local minimum on the potential energy surface.

To distinguish between *cis,gem*-**4c** and *trans,gem*-**4c** and to gauge the viability of these structures, we investigated the relative stabilities of *cis,gem*-**4c** and *trans,gem*-**4c** and also the *trans*- η^1,η^1 isomer $\eta^1,\eta^1\text{-}4$ and the *trans*- η^1,η^2 isomer $\eta^1,\eta^2\text{-}4\mathbf{c}$ computationally at the SMD(DCE)/TPSSh/aug-cc-pVTZ//B3LYP/6-31G(d) level of theory (Figure 7). Of the *gem*-diaurated structures, *cis,gem*-**4c** was nominally (1.2 kcal/mol) more stable than was *trans,gem*-**4c**. However, and in contrast to our expectations, these *gem*-diaurated structures were ≥ 12.6 kcal/mol less stable than was $\eta^1,\eta^2\text{-}4\mathbf{c}$, whereas $\eta^1,\eta^1\text{-}4\mathbf{c}$ did not represent a local minimum and instead collapsed to $\eta^1,\eta^2\text{-}4\mathbf{c}$ upon minimization. Rapid exchange of the π -bound gold atom between the two cyclopentadienyl C=C bonds of $\eta^1,\eta^2\text{-}4\mathbf{c}$ would be anticipated by analogy to mononuclear cationic gold η^2 -diene complexes.^{33,34} Conversely, it is difficult to envision a fluxional process that would account for both the time-averaged, two-fold symmetry of **4c** and the coupling of both $(\mathbf{P})\text{Au}$ groups to the cyclopentadienyl CH carbon atom as was established by NMR spectroscopy. Owing to the lack of congruency between the spectroscopy and computational modeling of **4c**, we refrain from assigning a defined structure to **4c**.

Relative binding affinities of mono(gold) cyclopentadienyl complexes. We sought to quantify the relative binding affinities of the mononuclear gold (η^1 -cyclopentadienyl) complexes **3a**–**3c** and the corresponding unmetallated cyclopentadienes toward exogenous $(\mathbf{P})\text{Au}^+$. Our objectives here were to (1) evaluate the effect of ring substitution on the binding affinity of gold η^1 -allyl complexes and (2) to gauge the effect of the σ -bound $(\mathbf{P})\text{Au}$ group on the binding affinity relative to the unmetallated cyclic hydrocarbon. To this end, we determined equilibrium constants for the displacement of the benzonitrile from $[(\mathbf{P})\text{Au}(\text{NCPh})]^+ \text{SbF}_6^-$ (**5**) with **3a**, **3b**, **3c**, C_5H_6 , $\text{C}_5\text{H}_5\text{Me}$, $\text{C}_5\text{H}_2\text{Me}_4$ in CD_2Cl_2 at -80°C employing ^{31}P NMR analysis (eq 1).³⁰



Binding of exogenous $(\mathbf{P})\text{Au}^+$ to gold cyclopentadienyl complexes **3a** and **3b** was highly favorable such that addition of **3a** or **3b** to a solution of **5** containing excess benzonitrile (55 mM) led to quantitative formation of bis(gold) complexes **4a** and **4b**, respectively. Assuming $\geq 5\%$ of **5** would have been detected by ^{31}P NMR analysis, we set lower limits for the equilibrium constants for displacement of benzonitrile from **5** by **3a** and **3b** of $K_{\text{eq}} \geq 400$ and $K_{\text{eq}} \geq 400$, respectively (Table 1, entries 1 and 2). In comparison, the binding affinity of tetramethylcyclopentadienyl complex **3c** toward $(\mathbf{P})\text{Au}^+$ ($K_{\text{eq}} = 8.6$) was ≥ 35 times less favorable than for complexes **3a** and **3b** (Table 1, entry 3). Nevertheless, the binding affinities of gold cyclopentadienyl complexes **3a**, **3b**, and **3c** toward $(\mathbf{P})\text{Au}^+$ exceeds the binding affinities of the corresponding unmetallated cyclopentadienes C_5H_6 ($K_{\text{eq}} = 4.3 \pm 0.8 \times 10^{-2}$), $\text{C}_5\text{H}_5\text{Me}$ ($K_{\text{eq}} = 0.22 \pm 0.02$), and $\text{C}_5\text{H}_2\text{Me}_4$ ($K_{\text{eq}} \leq 2.4 \times 10^{-3}$), respectively, by more than three orders of magnitude in each case (Table 1, entries 4–6).

Table 1. Equilibrium constants for the displacement of benzonitrile from $[(\mathbf{P})\text{Au}(\text{NCPh})]^+ \text{SbF}_6^-$ (**5**).

entry	L	$(\mathbf{P})\text{Au}(\text{L})^+$	K_{eq}
1	3a	4a	$\geq 400^{\text{a}}$
2	3b	4b	$\geq 400^{\text{a}}$

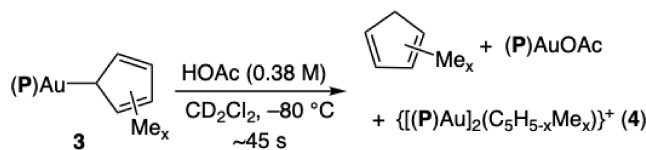
3	3c	4c	8.6 ± 0.6
4	C ₅ H ₆	(P)Au(π -C ₅ H ₆)	$(4.3 \pm 0.8) \times 10^{-2}$
5	C ₅ H ₅ Me	(P)Au(π -C ₅ H ₅ Me)	0.22 ± 0.02
6	C ₅ H ₂ Me ₄	(P)Au(π -C ₅ H ₂ Me ₄)	$\leq 2.4 \times 10^{-3}$ ^b

^aComplex **5** not detected at equilibrium. ^b π -Complex not detected at equilibrium.

The much higher binding affinity of the gold cyclopentadienyl complexes **3** relative to the corresponding unmetallated cyclopentadienes was expected given our previous studies on mono and bis(gold) indenyl complexes¹² and mono and bis(gold) gold alkynyl complexes,⁹ which also revealed higher LAu⁺ binding affinity of the gold σ -complex relative to the free hydrocarbon. In all these cases, the greater binding affinity of the gold σ -complexes compared to the unmetallated hydrocarbons is likely due to the greater σ -donor ability of the LAu group relative to hydrogen, resulting in the greater electron donating ability of the gold σ -complex as compared to the unmetallated hydrocarbon. Although the structure of the bis(gold) tetramethylcyclopentadienyl complex **4c** remains unclear, the greater affinity of **3a** and **3b** toward exogenous (P)Au⁺ relative to **3c** established the deleterious effect of the four cyclopentadienyl methyl groups on the stability of bis(gold) complex **4c**.

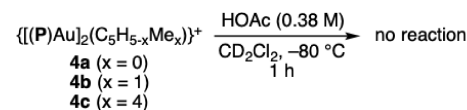
Protodeauration of gold cyclopentadienyl complexes. We also sought to evaluate the reactivity of bis(gold) cyclopentadienyl complexes **4** toward protodeauration relative to the corresponding mono(gold) complexes **3**. Treatment of monogold complexes **3a**, **3b**, or **3c** (~33 mM) with excess acetic acid (380 mM) in CD₂Cl₂ at -80 °C led, in each case, to complete consumption of **3** within ~45 s as judged by ³¹P NMR analysis. ¹H and ³¹P NMR analysis of the resulting solutions revealed formation of the corresponding cyclopentadiene as the exclusive organic product along with mixtures of (P)AuOAc and the corresponding bis(gold) complex **4** as the exclusive organometallic products. The ratio of (P)AuOAc:**4** was substrate dependent, ranging from (P)AuOAc:**4a** = 13:1 for the protodeauration of **3a**, (P)AuOAc:**4b** = 36:1 for the protodeauration of **3b**, and (P)AuOAc:**4c** = 3.3:1 for the protodeauration of **3c** (Table 2). Because the (P)AuOAc:**4** ratio does not track with the relative equilibrium binding affinities of **3** toward exogenous (P)Au⁺ (**3a/b** > **3c**), the (P)AuOAc:**4** ratio formed in the protodeauration of complexes **3** presumably reflects the kinetic selectivity. Assuming that (1) ≥10% of unreacted **3** would have been observed in the initial ³¹P NMR spectrum of the solution of **3** and HOAc and (2) protodeauration obeys pseudo first-order kinetics, we can set a lower limit for the observed rate constant for the protodeauration of complexes **3** of $k_{obs} \geq 5 \times 10^{-2}$ s⁻¹.

Table 2. Reaction of gold cyclopentadienyl complexes **3 (33 mM) with acetic acid (0.38 M) in CD₂Cl₂ at -80 °C.**



cmpd	x	(P)AuOAc: 4
3a	0	13.3
3b	1	35.8
3c	4	3.3

In comparison to the rapid protodeauration of mono(gold) cyclopentadienyl complexes **3**, protodeauration of bis(gold) cyclopentadienyl complexes **4** was sluggish. Treatment of the bis(gold) complexes **4a**, **4b**, or **4c** (33 mM) with HOAc (0.38 M) in CD₂Cl₂ at -80 °C revealed no detectable consumption of **4** after 1 h (Scheme 7). Conservatively assuming that ≥10% consumption of **4** would have been observed in the ¹H and ³¹P NMR spectra of solutions of **4** and HOAc and that protodeauration obeys pseudo first-order kinetics, we can set an upper limit for the observed rate constant for the protodeauration of complexes **4** of $k_{obs} \leq 3 \times 10^{-5}$ s⁻¹. Therefore, protodeauration of bis(gold) cyclopentadienyl complexes **4** is >1500 times slower than is protodeauration of the corresponding monogold cyclopentadienyl complexes **3** under identical conditions.



CONCLUSIONS

The neutral gold cyclopentadienyl complexes (P)Au(η^1 -C₅H₅) (**3a**) and (P)Au(η^1 -C₅H₄Me) (**3b**) react with (P)AuNTf₂ to form the cationic bis(gold) complexes *trans*-{[(P)Au]₂(η^1 , η^1 -cyclopentadien-1,3-yl)}⁺NTf₂⁻ (**4a**) and *trans*-{[(P)Au]₂(η^1 , η^1 -methylcyclopentadien-1,3-yl)}⁺NTf₂⁻ (**4b**), respectively, which were characterized in solution and the solid state. Complexes **4a** and **4b** are highly fluxional in solution at -80 °C with the gold atoms migrating about the cyclopentadienyl ring, presumably via sequential [1,5] sigmatropic rearrangement. In the solid-state, the gold atoms of **4a** and **4b** are positioned on opposite faces of the cyclopentadienyl ring above and below the C1 and C3 carbon atoms. The gold tetramethylcyclopentadienyl complex (P)Au(η^1 -C₅HMe₄) (**3b**) also reacts with (P)AuNTf₂ to form the cationic bis(gold) complex {[(P)Au]₂(C₅HMe₄)₂}⁺NTf₂⁻ (**4c**), although the structure of this complex was not firmly established.

The Au-C bond lengths and angles of **4a** (and also **4b**) are similar to those previously calculated for the *trans*- η^1 , η^1 -inden-1,3-yl complex **1a**, pointing to analogous orbital interactions in both complexes that, in the case of **4a**, presumably involves overlap of the symmetric combination of the P–Au anti-bonding orbitals [φ_a(σ*)] with the filled antisymmetric cyclopentadienyl 2π_b molecular orbital. This bonding model is similar to that proposed to describe the M–C bonding interactions in dinuclear palladium and nickel μ -allyl, μ -cyclopentadienyl and μ -indenyl complexes, but lacks the M→C backbonding interactions present in these latter complexes.^{18,19} Also worth noting is that computational analyses of these dinuclear Pd and Ni complexes support a common bonding model for μ -cyclopentadienyl, indenyl, and simple allyl ligands.¹⁹ In a similar way, the common bonding interaction of *trans*- η^1 , η^1 -cyclopentadienyl and indenyl gold complexes suggests that the *trans*- η^1 , η^1 bonding motif might also extend to simple gold allyl complexes, although this contention remains untested.

The mono(gold) cyclopentadienyl complexes **3a** and **3b** display higher (≥ 35-fold) binding affinity toward exogenous (P)Au⁺ than does the mono(gold) tetramethylcyclopentadienyl

complex **3c**, pointing to destabilization of bis(gold) complex **4c** by the four cyclopentadienyl methyl groups. Nevertheless, the binding affinities of the mono(gold) cyclopentadienyl complexes **3** toward exogenous **(P)Au⁺** exceed those of the corresponding unmetallated cyclopentadienes by more than three orders of magnitude, presumably due to the greater σ -donor ability of the **(P)Au** fragment relative to a hydrogen atom. The reactivity of the bis(gold) cyclopentadienyl complexes **4** toward protodeauration was more than three orders of magnitude lower than for the corresponding mono(gold) cyclopentadienyl complexes **3**. Both the aggregation behavior of mono(gold) cyclopentadienyl complexes **3** and the protodeauration behavior of cationic bis(gold) cyclopentadienyl complexes **4** mirror the reactivity of the corresponding indenyl complexes.¹² Although the extent to which this reactivity is similarly mirrored by simple gold allyl complexes has not been established, the high association constants of the mono(gold) cyclopentadienyl and indenyl complexes toward exogenous **LAu⁺** and sluggish protodeauration of the resulting cationic bis(gold) complexes points to the potential relevance of cationic bis(gold)allyl complexes in gold(I)-catalyzed processes that involve gold η^1 -allyl intermediates.

EXPERIMENTAL SECTION

[P(t-Bu)₂o-biphenyl]Au(η¹-C₅H₅) (3a). Cyclopentadiene (22 μ L, 0.27 mmol) was added via syringe to a solution of *n*-butyllithium (0.12 mL, 0.30 mmol, 2.5 M in hexanes) in THF (3 mL) at 0 °C and the solution was stirred for 1 h. A solution of **(P)AuOTf** (0.18 g, 0.27 mmol) in THF (3 mL) was added via syringe to the solution of cyclopentadienyl lithium at 0 °C and the resulting solution was stirred overnight at room temperature. The solvent was evaporated under vacuum and the residue was washed with hexane (3 \times 8 mL) to give a brown solid that was dissolved in CH₂Cl₂, filtered (0.22 mM mesh), and evaporated under vacuum to give **3a** (0.11 g, 70%) as a pale brown solid. Crystals suitable for X-ray diffraction were grown by slow diffusion of hexanes into a concentrated CH₂Cl₂ solution of **3a** at -20 °C. ¹H NMR (700 MHz, CD₂Cl₂, -80 °C): δ 7.75 (t, J = 7.31 Hz, 1H), 7.52 – 7.40 (m, 5H), 7.19 (d, J = 7.2 Hz, 3H), 5.54 (s, 5H), 1.08 (d, J = 15.2 Hz, 18H). ¹³C{¹H} NMR (176 MHz, CD₂Cl₂, -80 °C): δ 148.63 (d, J = 15.5 Hz), 142.60 (d, J = 6.1 Hz), 133.62, 132.01 (d, J = 7.5 Hz), 129.51, 129.14, 127.51, 126.74, 126.32 (d, J = 21.3 Hz), 126.04, 109.56 (d, J = 7.0 Hz), 35.57 (d, J = 22.0 Hz), 29.56. ³¹P{¹H} NMR (C CD₂Cl₂, 283 MHz, -80 °C): δ 61.61. HRMS (APCI/APPI) calcd (found) for C₂₅H₃₂AuP: 560.1924 (560.1907).

[P(t-Bu)₂o-biphenyl]Au(η¹-C₅H₄Me) (3b). Reaction of **(P)AuOTf** with C₅H₄MeLi employing a procedure analogous to that used to synthesize **3a** gave **3b** in 63% yield as a pale brown solid. ¹H NMR (700 MHz, CD₂Cl₂, -80 °C): δ 7.75 (t, J = 7.21 Hz, 1H), 7.49 – 7.41 (m, 5H), 7.18 (s, 3H), 5.22 (s, 2H), 5.05 (s, 2H), 1.99 (s, 3H), 1.10 (d, J = 15.4 Hz, 18H). ¹³C{¹H} NMR (176 MHz, CD₂Cl₂, -80 °C): δ 149.4 (d, J = 15.7 Hz), 143.4 (d, J = 5.7 Hz), 134.5, 134.3, 132.7 (d, J = 6.9 Hz), 130.2, 129.8, 128.3, 127.4, 127.3, 127.1, 109.0 (m), 107.0 (m), 36.5 (d, J = 21.4 Hz), 30.3 (br s), 16.2. ³¹P{¹H} NMR (CD₂Cl₂, 283 MHz, -80 °C): δ 62.06. HRMS (APCI/APPI) calcd (found) for C₂₆H₃₄AuP: 574.2082 (574.2064).

[P(t-Bu)₂o-biphenyl]Au(η¹-C₅HMe₄) (3c). Reaction of **(P)AuOTf** with C₅HMe₄Li employing a procedure analogous to that used to synthesize **3a** gave **3c** in 60% yield as a brown solid. ¹H NMR (700 MHz, CD₂Cl₂, -80 °C): δ 7.82 (t, J = 7.85 Hz, 1H), 7.49 – 7.36 (m, 5H), 7.16 (m, 3H), 2.12 (d, J = 14.8 Hz, 1H), 1.73 (s, 6H), 1.68 (s, 6H), 1.21 (d, J = 14.8 Hz, 18H). ¹³C{¹H} NMR (176 MHz, CD₂Cl₂, -80 °C): δ 148.86 (d, J = 16.5 Hz), 143.58 (d, J = 5.6 Hz), 134.58, 133.87, 132.17 (d, J = 7.7 Hz), 129.32, 128.94, 128.21, 128.02, 127.58, 126.77, 126.26 (d, J = 5.1 Hz), 126.10 (d, J = 3.0 Hz), 71.19 (d, J = 61.3 Hz), 36.41 (d, J = 19.5 Hz), 29.94, 14.17, 11.00. ³¹P{¹H} NMR (CD₂Cl₂, 283 MHz, -80 °C): δ 64.14. HRMS (APCI/APPI) calcd (found) for C₂₉H₄₀AuP: 616.2553 (616.2533).

{[P(t-Bu)₂o-biphenyl]Au₂(η¹,η¹-1,3-C₅H₅)⁺NTf₂⁻ (4a). A solution of **3a** (15 mg, 4.5 \times 10⁻² mmol) and **(P)AuNTf₂** (21 mg, 4.5 \times 10⁻² mmol) in CD₂Cl₂ (600 μ L) was added to NMR tube, shaken, and cooled to -80 °C. ³¹P NMR analysis of the solution revealed quantitative (\geq 98%) formation of **4a**. Slow diffusion of hexanes into the resulting solution at -20 °C for 12 h gave **4a** (34 mg, 95%) as yellow-brown crystals. ¹H NMR (700 MHz, CD₂Cl₂, -80 °C): δ 7.74 (t, J = 7.60 Hz, 2H), 7.55-7.41 (m, 10H), 7.24-7.12 (m, 6H), 5.43 (s, 5H), 1.07 (d, J = 15.8 Hz, 36H). ¹³C{¹H} NMR (176 MHz, CD₂Cl₂, -80 °C): δ 148.11 (d, J = 14.3 Hz), 142.52 (d, J = 6.8 Hz), 133.17, 132.15 (d, J = 7.7 Hz), 130.08, 129.27, 127.94, 126.74 (d, J = 28.9 Hz), 124.56, 124.31, 118.9 (q, J_{CF} = 320 Hz), 107.95, 35.84 (d, J = 24.0 Hz), 29.49. ³¹P{¹H} NMR (CD₂Cl₂, 283 MHz, -80 °C): δ 60.15.

{[P(t-Bu)₂o-biphenyl]Au₂(η¹,η¹-1,3-C₅H₄Me)⁺NTf₂⁻ (4b). A solution of **3b** (15 mg, 4.4 \times 10⁻² mmol) and **(P)AuNTf₂** (20 mg, 4.3 \times 10⁻² mol) in CD₂Cl₂ (600 μ L) was added to NMR tube, shaken, and cooled to -80 °C. ³¹P NMR analysis of the solution revealed quantitative (\geq 97%) formation of **4b**. Slow diffusion of hexanes into the resulting solution at -20 °C for 12 h gave **4b** (27 mg, 96%) as yellow-brown crystals. ¹H NMR (700 MHz, CD₂Cl₂, -80 °C): δ 7.74 (t, J = 7.8 Hz, 2H), 7.53 – 7.41 (m, 10H), 7.22-7.13 (m, 6H), 5.13 (s, 2H), 4.80 (s, 2H), 1.94 (s, 3H), 1.08 (d, J = 15.5 Hz, 36H). ¹³C{¹H} NMR (176 MHz, CD₂Cl₂, -80 °C): δ 148.9 (d, J = 14.7 Hz), 143.3 (d, J = 6.5 Hz), 141.7, 133.9, 132.8 (d, J = 7.8 Hz), 130.8, 129.9, 128.7, 127.5 (d, J = 6.2 Hz), 127.2, 125.2 (d, J = 42.9 Hz), 119.58 (q, J_{CF} = 321 Hz), 103.7 (m), 103.6 (m), 36.7 (d, J = 23.7 Hz), 30.2 (br s), 15.7. ³¹P{¹H} NMR (CD₂Cl₂, 283 MHz, -80 °C): δ 60.44.

{[P(t-Bu)₂o-biphenyl]Au₂(C₅HMe₄)⁺NTf₂⁻ (4c). A solution of **3c** (15 mg, 0.02 mmol) and **(P)AuNTf₂** (19 mg, 0.02 mmol) in CD₂Cl₂ (600 μ L) was added to NMR tube, shaken, and cooled to -80 °C. ³¹P NMR analysis of the solution revealed formation of **4c** which constituted $>90\%$ of the reaction mixture. ¹H NMR (700 MHz, CD₂Cl₂, -80 °C): δ 7.76 (t, J = 7.89 Hz, 2H), 7.47 (s, 10H), 7.12 (s, 6H), 3.18 (s, 1H), 1.79 (s, 6H), 1.56 (s, 6H), 1.08 (d, J = 15.4 Hz, 36H). ¹³C{¹H} NMR (176 MHz, CD₂Cl₂, -80 °C): δ 148.35 (d, J = 14.6 Hz), 142.58 (d, J = 6.3 Hz), 134.29, 133.47, 132.40 (d, J = 7.6 Hz), 130.08, 129.07, 127.89, 126.93, 126.65, 124.44, 124.21, 118.9 (q, J_{CF} = 320 Hz), 116.21, 85.07 (t, J = 17.0 Hz), 36.54 (d, J = 23.3 Hz), 29.51, 15.31, 12.00. ³¹P{¹H} NMR (CD₂Cl₂, 283 MHz, -80 °C): δ 60.41.

Equilibrium binding affinity of gold cyclopentadienyl complexes to **(P)Au⁺.** A solution of **3a** (6 mg, 0.01 mmol) and **[(P)Au(NCPh)]⁺SbF₆⁻** (**5**; 9 mg, 0.01 mol) in CD₂Cl₂ (600 μ L) containing benzonitrile (\sim 55 mM) was added to an NMR tube, mixed thoroughly, and placed in the probe of an NMR spectrometer precooled at -80 °C. ³¹P NMR analysis of the solution showed quantitative conversion of **5** to **4a**. Assuming that $\geq 5\%$ of **5** would have been detected in solution, a lower limit for the equilibrium constant for the conversion of **3a** and **5** to **4a** and NCPh of $K_{eq} = [4a][NCPh]/[3a][5] \geq 400$ was determined assuming [NCPh] = [4a]. Employing similar procedures and assumptions, equilibrium constants for the conversion of **3b** and **5** to **4b** ($K_{eq} = [4b][NCPh]/[3b][5] \geq 400$) and for the conversion of **3c** and **5** to **4c** ($K_{eq} = [4c][NCPh]/[3c][5] = 8.63$) were determined.

Equilibrium binding affinity of cyclopentadienes to **(P)Au⁺.** A solution of cyclopentadiene (1.5 μ L, 0.02 mmol) and **[(P)Au(NCPh)]⁺SbF₆⁻** (**5**; 15 mg, 0.02 mmol) in CD₂Cl₂ (600 μ L) was added to an NMR tube, mixed thoroughly, and placed in the probe of an NMR spectrometer precooled at -80 °C. ³¹P NMR analysis of the solution revealed a 1.0:4.7 mixture of **[(P)Au(η²-C₅H₆)⁺SbF₆⁻** (**6a**) and **5**; **6a** was characterized in solution by ¹H and ³¹P NMR spectroscopy and by analogy to known cationic **(P)Au(η²-1,3-diene)** complexes.^{32,33} An equilibrium constant for the conversion of **5** to **6a** of $K_{eq} = [6a][NCPh]/[C_5H_6][5] = 0.043 \pm 0.008$ was determined assuming [C₅H₆] = [5] and [NCPh] = [6a]. Employing a similar procedure and assumptions, an equilibrium constant for the reaction of methylcyclopentadiene with **5** of $K_{eq} = [(6b)][NCPh]/[C_5H_5Me][5] = 0.22 \pm 0.02$ was determined where **6b** = **[(P)Au(η²-C₅H₅Me)⁺SbF₆⁻**. ³¹P NMR analysis of an equimolar solution of **5** and 2,4,5,6-tetramethylcyclopentadiene revealed no detectable formation of **[(P)Au(η²-C₅H₂Me₄)⁺SbF₆⁻** (**6c**). Assuming $\geq 5\%$ of **6c** would have been detected in solution, an upper limit for the

equilibrium constant for the reaction of $C_5H_2Me_4$ with **5** of $K_{eq} = [(6c)][NCPH]/[C_5H_2Me_4][5] \leq 2.4 \times 10^{-3}$ was determined

For (P)Au(π -C₅H₆) (6a):³³ 1H NMR (CD₂Cl₂, 700 MHz, -80 °C): δ 7.93–7.01 (m), 6.80 (br s, 2H), 5.79 (br s, 2H), 3.25 (d, $J = 25.7$ Hz, 1H), 3.14 (d, $J = 26.1$ Hz, 1H) 1.27 (d, $J = 16.7$ Hz, 18H). $^{31}P\{^1H\}$ NMR (CD₂Cl₂, 283 MHz, -80 °C): δ 62.95.

For (P)Au(π -C₅H₅Me) (6b): 1H NMR (CD₂Cl₂, 700 MHz, -80 °C): δ 7.93–7.02 (m), 6.40 (s, 1H), 6.31 (s, 1H), 5.37 (s, 1H), 3.06 (d, $J = 12.5$ Hz, 2H), 2.05 (s, 3H), 1.21 (d, $J = 16.67$ Hz, 18H). $^{31}P\{^1H\}$ NMR (CD₂Cl₂, 283 MHz, -80 °C): δ 63.08.

Protodeauration of 3a, 3b, and 3c. Acetic acid (12 μ L, 0.20 mmol) was added to an NMR tube containing a solution of **3a** (12 mg, 0.020 mmol) in CD₂Cl₂ (600 μ L) at -80°C. The contents of the tube were mixed thoroughly and placed in the probe of an NMR spectrometer precooled at -80°C. A ^{31}P NMR spectrum recorded within 45 s revealed complete consumption of **3a** to form a 1:13 mixture of **4a** and (P)AuOAc as the only phosphorus-containing species; (P)AuOAc was identified by comparison to an authentic sample. The 1H NMR spectrum recorded immediately thereafter revealed formation of a ~36:1 mixture of free cyclopentadiene and **4a** as the exclusive cyclopentadiene containing species. Assuming that $\geq 10\%$ of unreacted **3a** would have been observed in the initial ^{31}P NMR spectrum and the protodeauration of **3a** obeys pseudo first-kinetics, we set a lower limit for the observed rate constant for protodeauration of **3a** of $k_{obs} \geq 5 \times 10^{-2}$ s $^{-1}$. Employing similar procedures and assumptions, we set lower limits for the observed rate constant for protodeauration of **3b** and **3c** of $k_{obs} \geq 5 \times 10^{-2}$ s $^{-1}$. Protodeauration of **3b** formed (P)AuOAc and methylcyclopentadiene, which comprised $> 95\%$ of the organic and organometallic reaction products, respectively. Protodeauration of **3c** formed a 1.0:3.3:0.67 mixture of **4c**:(P)AuOAc: $C_5H_2Me_4$.

(P)AuOAc. A solution of (P)AuCl (50 mg, 0.09 mmol) and AgOAc (16 mg, 0.09 mmol) in CH₂Cl₂ (3 mL) was stirred at room temperature for ~1 hr. The solution was filtered and concentrated under reduced pressure to give (P)AuOAc (43 mg, 83%) as a white solid. $^{31}P\{^1H\}$ NMR (CD₂Cl₂, 283 MHz, -80 °C): δ 53.90.

Protodeauration of 4a, 4b, and 4c. In three separate experiments, acetic acid (13 μ L, 0.23 mmol) was added to a solution of **4a**, **4b**, or **4c** (~0.02 mmol) in CD₂Cl₂ (600 μ L) at -80 °C. The contents of the tube were mixed thoroughly and placed in the probe of an NMR spectrometer precooled at -80°C. ^{31}P and 1H NMR analysis of the solutions recorded after 1 h revealed no detectable consumption of **4**. Assuming that $\geq 10\%$ consumption of **4** would have been observed in the ^{31}P NMR spectrum and protodeauration of **4** obeys pseudo first-order kinetics, we can set an upper limit for the observed half-life for protodeauration of $k_{obs} \leq 3 \times 10^{-5}$ s $^{-1}$.

Computational methods. All DFT calculations were performed employing the Gaussian 16 program.³⁵ The B3LYP method³⁶ was used to locate all relevant conformations. The def2-TZVPP basis set was applied for all the nonmetallic atoms and def2ECP pseudopotential with the corresponding def2-TZVPP basis set was applied for gold. All the stationary points were optimized in the gas-phase and frequency calculations were performed at the same level to evaluate the thermal corrections at 298 K without scaling. Conformational energies based on the geometry structures obtained at the B3LYP level were calculated using the def2-TZVPP basis set for nonmetallic atoms and def2ECP pseudopotential with the corresponding def2-TZVPP basis set for gold.

ASSOCIATED CONTENT

Supporting Information

The Supporting Information is available free of charge on the ACS Publications website.

Synthetic procedures, computational details, and scans of NMR spectra

AUTHOR INFORMATION

Corresponding Author

Ross A. Widenhoefer – Department of Chemistry, Duke University, Durham, North Carolina 27708, United States; orcid.org/0000-0002-5349-8477; Email: rwidenho@chem.duke.edu

Authors

Brady L. Slinger – Department of Chemistry, French Family Science Center, Duke University, Durham, North Carolina 27708, United States

Jack C. Malek – Department of Chemistry, French Family Science Center, Duke University, Durham, North Carolina 27708, United States

ACKNOWLEDGMENTS

This work was supported by the NSF (CHE-2102653). Crystallographic work was supported by the National Science Foundation under grant no. CHE-2117287. We thank William Hearne and Josh Chen (UNC-Chapel Hill) for performing the X-ray crystallography of complexes **3a**, **4a**, and **4b** and for thoughtful discussions. We also thank a reviewer for suggesting a rationale for the large J_{CP} observed for cyclopentadienyl CH resonance of complex **3c**. The authors declare no competing financial interests.

REFERENCES

- (1) (a) Weber, D.; Gagné, M. R. Auophilicity in gold(I) catalysis: for better or worse? *Top. Curr. Chem.* **2014**, *357*, 167–212. (b) Bayrakdar, T. A. C. A.; Scattolin, T.; Maa, X.; Nolan, S. P. Dinuclear gold(I) complexes: from bonding to applications. *Chem. Soc. Rev.* **2020**, *49*, 7044–7100.
- (2) Seidel, G.; Lehmann, C. W.; Fürstner, A. Elementary Steps in Gold Catalysis: The Significance of *gem*-Diauration. *Angew. Chem. Int. Ed.* **2010**, *49*, 8466 – 8470.
- (3) Zhdanko, A.; Maier, M. E. Synthesis of *gem*-Diaurated species from Alkynols. *Chem. Eur. J.* **2013**, *19*, 3932–3942.
- (4) Weber, D.; Gagné, M. R. σ - π -Diauration as an alternative binding mode for digold intermediates in gold(I) catalysis. *Chem Sci.* **2013**, *4*, 335–338.
- (5) (a) Brown, T. J.; Weber, D.; Gagné, M. R.; Widenhoefer, R. A. Mechanistic analysis of gold(I)-catalyzed intramolecular allene hydroalkoxylation reveals an off-cycle bis(gold) vinyl species and reversible C–O bond formation. *J. Am. Chem. Soc.* **2012**, *134*, 9134–9137. (b) Weber, D.; Tarselli, M. A.; Gagné, M. R. Mechanistic Surprises in the Gold(I)-Catalyzed Intramolecular Hydroarylation of Alkenes. *Angew. Chem. Int. Ed.* **2009**, *48*, 5733–5736. (c) Tang, Y.; Li, J.; Zhu, Y.; Li, Y.; Yu, B. Mechanistic insights into the Gold(I)-catalyzed Activation of Glycosol ortho-alkynylbenzoates for Glycosidation. *J. Am. Chem. Soc.* **2013**, *135*, 18396–18405. (d) Zhdanko, A.; Maier, M. E. The Mechanism of Gold(I)-Catalyzed Hydroalkoxylation of Alkynes: An Extensive Experimental Study. *Chem. Eur. J.* **2014**, *20*, 1918–1930.
- (6) (a) Nesmeyanov, A. N.; Perevalova, E. G.; Grandberg, K. I.; Lemovskii, D. A.; Baukova, T. V.; Afanassova, O. B. A new type of organogold compound. *J. Organomet. Chem.* **1974**, *65*, 131–144. (b) Weber, D.; Jones, T. D.; Adduci, L. L.; Gagné, M. R. Strong Electronic and Counterion Effects on Geminal Digold Formation and Reactivity as Revealed by Gold(I)-Aryl Model Complexes. *Angew. Chem. Int. Ed.* **2012**, *51*, 2452 –2456. (c) Nesmeyanov, A. N.; Perevalova, E. G.; Grandberg, K. I.; Lemovskii, D. A. Organogold Complexes. *Izv. Akad. Nauk SSSR Ser. Khim.* **1974**, *5*, 1124–1137. (d) Osawa, M.; Hoshino, M.; Hashizume, D. Photoluminescent properties and molecular structures of [NaphAu(PPh₃)] and [μ -Naph{Au(PPh₃)₂} ClO₄ (Naph = 2-naphthyl)]. *Dalton Trans.* **2008**, 2248–2252. (e) Uson, R.; Laguna, A.; Fernandez, E. J.; Media, A.; Jones, P. G. (Polyhalophenyl)silver(I) complexes as arylating agents: Crystal structure of [(μ -2,4,6-C₆F₃H₂)(AuPPh₃)₂]ClO₄. *J. Organomet. Chem.* **1988**, *350*, 129–138. (f) Schmidbaur, H.; Inoguchi, Y. Cyclische μ -(4-Methylcyclohexadien-1-ylidenio)-bis[phosphangold(I)]-Kationen. *Chem. Ber.* **1980**, *113*, 1646–1653. (g) Heckler, J. E.; Zeller, M.; Hunter, A. D.; Gray, T. G.

Geminally Diaurated Gold(I) Aryls from Boronic Acids. *Angew. Chem. Int. Ed.* **2012**, *51*, 5924–5928.

(7) Porter, K. A.; Schier, A.; Schmidbaur, H. Auration of Thiophene and Furan: Structures of the 2-Mono-and 2,2-Diaurated Products. *Organometallics* **2003**, *22*, 4922–4927.

(8) (a) Schmidbaur, H.; Schier, A. Auophilic interactions as a subject of current research: an up-date. *Chem. Soc. Rev.* **2012**, *41*, 370–412. (b) Schmidbaur, H.; Schier, A. A briefing on auophilicity. *Chem. Soc. Rev.* **2008**, *37*, 1931–1951. (c) Schmidbaur, H. The auophilicity phenomenon: A decade of experimental findings, theoretical concepts, and emerging applications. *Gold Bull.* **2000**, *33*, 3–10. (d) Schmidbaur, H. Ludvig Mond Lecture. High-carat gold compounds. *Chem. Soc. Rev.* **1995**, *24*, 391–400.

(9) (a) Brown, T. J.; Widenhoefer, R. A. Cationic gold(I) π -complexes of terminal alkynes and their conversion to dinuclear σ,π -acetylide complexes. *Organometallics* **2011**, *30*, 6003–6009. (b) Grirrane, A.; Garcia, H.; Corma, A.; Alvarez, E. Intermolecular [2+2] Cycloaddition of Alkyne-Alkene Catalyzed by Au(I) Complexes. What are the Catalytic Sites Involved? *ACS Catal.* **2011**, *1*, 1647–1653.

(10) (a) Simonneau, A.; Jaroschik, F.; Lesage, D.; Karanik, M.; Guillot, R.; Malacria, M.; Tabet, J. C.; Goddard, J. P.; Fensterbank, L.; Gandon, V.; Gimbert, Y. Tracking gold acetylides in gold(I)-catalyzed cycloisomerization reactions of enynes. *Chem. Sci.* **2011**, *2*, 2417–2422. (b) Obradors, C.; Echavarren, A. M. Intermolecular Gold-Catalyzed Cycloaddition of Alkynes with Oxoalkenes. *Chem. Eur. J.* **2013**, *19*, 3547–3551. (c) Homs, A.; Obradors, C.; Leboeuf, D.; Echavarren, A. M. Dissecting Anion Effects in Gold(I)-catalyzed Intermolecular Cycloadditions. *Adv. Synth. Catal.* **2014**, *356*, 221–228. (d) Grirrane, A.; Garcia, H.; Corma, A.; Alvarez, E. Air-stable, Dinuclear, and Tetranuclear σ,π -acetylide Gold(I) Complexes and their Catalytic Implications. *Chem. Eur. J.* **2013**, *19*, 12239–12244.

(11) Zhdanko, A.; Maier, M. E. Quantitative Evaluation of the Stability of gem-diaurated species in Reactions with Nucleophiles. *Organometallics* **2013**, *32*, 2000–2006.

(12) Slinger, B.; Zhu, J.; Widenhoefer, R. A. Cationic Bis(gold) Indenyl Complexes. *ChemPlusChem* **2024**, *89*, e202300691.

(13) (a) Jackson, G. E.; Moss, J. R.; Scott, L. G. Fluxional behavior of the complex $\{[\eta^5\text{-C}_5\text{H}_5\text{Fe}(\text{CO})_2]_2[\mu\text{-C}_3\text{H}_5]\}^+ \text{PF}_6^-$ in solution. *S. Afr. J. Chem.* **1983**, *36*, 69–72. (b) Raper, G.; McDonald, W. S. The crystal structure of allylchloroplatinum. *Chem. Comm.* **1970**, 655. (c) McDonald, W. S.; Mann, B. E.; Raper, G.; Shaw, B. L.; Shaw, G. Some allyl complexes of platinum(II). *Chem. Comm.* **1969**, 1254–1255. (d) Mann, B. E.; Shaw, B. L.; Shaw, G. Transition metal–carbon bonds. Part XXVI. Allylic and olefin complexes of platinum(II). *J. Chem. Soc. A.* **1971**, 3536–3544. (e) Hughes, R. P.; Powell, J. The dynamic stereochemistry of the allylic ligand in a μ -allylic complex of platinum(II). *J. Organomet. Chem.* **1973**, *55*, C45–C48. (f) Gracey, B. P.; Mann, B. E.; Spencer, C. M. The fluxional behavior of $\text{Pt}_2(\eta^1,\eta^2\text{-C}_3\text{H}_5)_2(\text{acac})_2$. *J. Organomet. Chem.* **1985**, *297*, 375–378. (g) Hüffer, S.; Wieser, M.; Polborn, K.; Beck, W. Kohlenwasserstoffverbrückte komplexe: XXIX–XXXVIII. Mitteilung siehe Lit. 1. Nucleophile addition von carbonylmallaten an kationische allyl- und alken-komplexe von wolfram, mangan, rhodium, eisen, ruthenium, osmium, cobalt, und iridium: zwei-, drei-, und vierkernige komplexe mit σ,π -allyl- und σ,σ -alken-brücken. *J. Organomet. Chem.* **1994**, *481*, 45–55. (h) Müller, H. J.; Nagel, U.; Beck, W. Organometallic Lewis acids. 28. Directed synthesis of σ,π -allyl-bridged metal compounds via nucleophilic attack of carbonylmallates to cationic π -allyl complexes ($\eta^5\text{-C}_5\text{H}_5(\text{OC})(\text{ON})(\sigma,\pi\text{-allyl})\text{M}(\text{CO})$ ($\text{M} = \text{Re}, \text{Mn}$). *Organometallics* **1987**, *6*, 193–194. (i) Lotz, S.; Van Rooyen, P. H.; Meyer, R. σ,π -Bridging Ligands in Bimetallic and Trimetallic Complexes. *Adv. Organomet. Chem.* **1995**, *37*, 219–320.

(14) Einstein, F. W. B.; Gilbert, M.; Tuck, D. G. A. Cyclopentadienyl Bridge. The Crystal Structure of Tris(cyclopentadienyl)indium(III) at -100°. *Inorg. Chem.* **1972**, *11*, 2832–2836.

(15) Atwood, J. L.; Smith, K. D. The Nature of the Scandium–Carbon Bond. II. Crystal and Molecular Structure of Tricyclopentadienylscandium. *J. Am. Chem. Soc.* **1973**, *95*, 1488–1491.

(16) Bünder, W.; Weiss, E. The Crystal Structure of Bis(cyclopentadienyl)manganese, a Polymeric Compound with Cyclopentadienyl Bridges. *Z. Naturforsch.* **1978**, *33b*, 1235–1237.

(17) Mertz, K.; Zettler, F.; Hausen, H. D.; Weidlein, J. Die Kristallstruktur von $(\text{CH}_3)_2\text{GaC}_5\text{H}_5$. *J. Organomet. Chem.* **1976**, *122*, 159–170.

(18) (a) Werner, H. Novel Types of Metal–Metal Bonded Complexes Containing Allyl and Cyclopentadienyl Bridging Ligands. *Adv. Organomet. Chem.* **1981**, *19*, 155–182. (b) Tanase, T.; Nomura, T.; Yamamoto, Y.; Kobayashi, K. J. Synthesis and characterization of binuclear palladium complexes of isocyanides with novel bridging η^3 -indenyl ligands. Crystal structure of $[\text{Pd}_2(\mu\text{-}\eta^3\text{-indenyl})_2(\text{RNC})_2](\text{R} = 2,6\text{-dimethylphenyl})$. *J. Organomet. Chem.* **1991**, *410*, C25–C28. (c) Tanase, T.; Nomura, T.; Fukushima, T.; Yamamoto, Y.; Kobayashi, K. Studies on interactions of isocyanide with transition metal complexes. 36. Synthesis and characterization of a binuclear palladium(I) complex with bridging η^3 -indenyl ligands, $\text{Pd}_2(\mu\text{-}\eta^3\text{-indenyl})_2(\text{isocyanide})_2$, and its transformation to a tetrานuclear palladium(I) cluster of isocyanides, $\text{Pd}_4(\mu\text{-acetate})_4(\mu\text{-isocyanide})_4$. *Inorg. Chem.* **1993**, *32*, 4578–4584. (d) Sakaki, S.; Takeuchi, K.; Sugimoto, M.; Kurosawa, H. Geometries, Bonding Nature, and Relative Stabilities of Dinuclear Palladium(I) π -Allyl and Mononuclear Palladium(II) π -Allyl Complexes. A Theoretical Study. *Organometallics* **1997**, *16*, 2995–3003. (e) Hazari, N.; Hruszkewycz, D. P. Dinuclear Pd^{I} complexes with bridging allyl and related ligands. *Chem. Soc. Rev.* **2016**, *45*, 2871–2899.

(19) (a) Zhu, L.; Kostic, N. M. Molecular Orbital Study of Bimetallic Complexes Containing Conjugated and Aromatic Hydrocarbons as Bridging Ligands. *Organometallics* **1988**, *7*, 665–669. (b) Kurosawa, H.; Hirako, K.; Natsume, S.; Ogoshi, S.; Kanehisa, N.; Kai, Y.; Sakaki, S.; Takeuchi, K. New Insights into Structures, Stability, and Bonding of μ -Allyl Ligands Coordinated with Pd–Pd and Pd–Pt Fragments. *Organometallics* **1996**, *15*, 2089–2097. (c) Chalkley, M. J.; Guard, L. M.; Hazari, N.; Hofmann, P.; Hruszkewycz, D. P.; Schmeier, T. J.; Takase, M. K. Synthesis, Electronic Structure, and Reactivity of Palladium(II) Dimers with Bridging Allyl, Cyclopentadienyl, and Indenyl Ligands. *Organometallics* **2013**, *32*, 4223–4238. (d) Mecheri, S.; Zouchoune, B.; Zendaoui, S. M. Bonding and electronic structures in dinuclear ($\text{X}[(\text{Ind})\text{M}_2\text{L}_2]$ complexes ($\text{M} = \text{Ni}, \text{Pd}, \text{L} = \text{CO}, \text{PEt}_3, \text{X} = \text{Cl}, \text{Allyl}, \text{Ind} = \text{indenyl}, \text{Cp} = \text{cyclopentadienyl}$): analogy between four-electron donor ligands. *Theor. Chem. Acc.* **2020**, *139*, 12.

(20) (a) Beck, R.; Johnson, S. A. Dinuclear Ni(I)–Ni(I) Complexes with Syn-facial Bridging Ligands from Ni(I) Precursors or Ni(II)/Ni(0) Comproportionation. *Organometallics* **2013**, *32*, 2944–2951. (b) Wu, J.; Nova, A.; Balcells, D.; Brudvig, G. W.; Dai, W.; Guard, L. M.; Hazari, N.; Lin, P. H.; Pokhrel, R.; Takase, M. K. Nickel(I) Monomers and Dimers with Cyclopentadienyl and Indenyl Ligands. *Chem. Eur. J.* **2014**, *20*, 5327–5337.

(21) (a) Singh, R. R.; Liu, R. S. Gold-catalyzed imination/Mannich reaction cascades of 3-en-1-ynamides with anilines and aldehydes to enable 1,5-nitrogen functionalizations. *Adv. Synth. Catal.* **2016**, *358*, 1421–1427. (b) Uemura, M.; Watson, I. D. G.; Katsukawa, M.; Toste, F. D. Gold(I)-catalyzed enantioselective synthesis of benzopyrans via rearrangement of allylic oxonium intermediates. *J. Am. Chem. Soc.* **2009**, *131*, 3464–3465. (c) Shapiro, N. D.; Toste, F. D. Synthesis of azepines by a gold-catalyzed intermolecular [4 + 3]-annulation. *J. Am. Chem. Soc.* **2008**, *130*, 9244–9245. (d) Alcaide, B.; Almendros, P.; Quirós, M. T.; Fernández, I.; Beilstein. *J. Org. Chem.* **2013**, *9*, 818–826. (e) Yeh, M. C. P.; Pai, H. F.; Lin, Z. J.; Lee, B. R. Stereoselective synthesis of hexahydroindoles and octahydrocyclohepta-[b]pyrroles via gold(I)-catalyzed intramolecular 1,4-hydroamination of cyclic 1,3-dienes. *Tetrahedron* **2009**, *65*, 4789–4794. (f) Young, P. C.; Hadfield, M. S.; Arrowsmith, L.; Macleod, K. M.; Mudd, R. J.; Jordan-Hore, J. A.; Lee, A. L. Divergent outcomes of gold(I)-catalyzed indole additions to 3,3-disubstituted cyclopropenes. *Org. Lett.* **2012**, *14*, 898–901. (g) Jimenez-Nunez, E.; Raducan, M.; Lauterbach, T.; Molawi, K.; Solorio, C. R.; Echavarren, A. M. Synthesis of (+)-Schisanwilsonene A by Tandem Gold-Catalyzed Cyclization/1,5-Migration/Cyclopropanation. *Angew. Chem. Int. Ed.* **2009**, *48*, 6152–6155. (h) Bauer, J. T.; Hadfield, M. S.; Lee, A. L. Gold catalysed reactions with cyclopropenes. *Chem. Commun.* **2008**, *44*, 6405–6407. (i) Hadfield, M. S.; Bauer, J. T.; Glen, P. E.; Lee, A. L. Gold(I)-catalyzed alcohol additions to cyclopropenes. *Org. Biomol. Chem.* **2010**, *8*, 4090–4095. (j) Mudd, R. J.; Young, P. C.; Jordan-Hore, J. A.; Rosair, G. M.; Lee, A. L. Gold(I)-Catalyzed Addition of Thiols and Thioacids to 3,3-Disubstituted Cyclopropenes. *J. Org. Chem.* **2012**, *77*, 7633–7639. (k) Watanabe, T.; Oishi, S.; Fujii,

N.; Ohno, H. Gold-catalyzed hydroarylation of allenes: a highly regioselective carbon–carbon bond formation producing six-membered rings. *Org. Lett.* **2007**, *9*, 4821–4824. (l) Cheng, X.; Zhu, L.; Lin, M.; Chen, J.; Huang, X. Rapid access to cyclopentadiene derivatives through gold-catalyzed cycloisomerization of ynamides with cyclopropenes by preferential activation of alkenes over alkynes. *Chem. Commun.* **2017**, *53*, 3745–3748. (m) Li, C.; Zeng, Y.; Zhang, H.; Feng, J.; Zhang, Y.; Wang, J. Gold(I)-catalyzed cycloisomerizations of enynes containing cyclopropenes. *Angew. Chem., Int. Ed.* **2010**, *49*, 6413–6417. (n) Meng, X.; Guo, M.; Zhu, J.; Zhu, H.; Sun, X.; Tian, L.; Cao, Z. Gold and TFOH-Cocatalyzed Tandem Reaction of ortho-alkynylarlyaldehydes with Cyclopropenes: an Efficient Route to Functionalized Benzo[7]annulene Derivatives. *Eur. J. Org. Chem.* **2019**, *2019*, 1952–1956. (o) Li, D.; Zang, W.; Bird, M. J.; Hyland, C. J. T.; Shi, M. Gold-catalyzed conversion of highly strained compounds. *Chem. Rev.* **2021**, *121*, 8478–8558.

(22) Dupuy, S.; Slawin, A. M. Z.; Nolan, S. P. The Fluoride-Free Transmetalation of Organosilanes to Gold. *Chem. Eur. J.* **2012**, *18*, 14923–14928.

(23) O'Brien, L.; Argent, S. P.; Ermanis, K.; Lam, H. W. Gold(I)-Catalyzed Nucleophilic Allylation of Azinium Ions with Allylboronates. *Angew. Chem. Int. Ed.* **2022**, *61*, e202202305.

(24) (a) Struchkov, Y. T.; Slovokhotov, Y. L.; Kravtsov, D. N.; Baukova, T. V.; Perevalova, E. G.; Grandberg, K. J. Characteristic structural features of cyclopentadienyl derivatives of post-transition metals: III. Synthesis and structure of fluorenyl (triphenylphosphine) gold (I). *J. Organomet. Chem.* **1988**, *338*, 269–280. (b) Baukova, T. V.; Slovokhotov, Y. L.; Struchkov, Y. T. Characteristic structural features of post-transition metal cyclopentadienyl derivatives: I. Tetraphenylcyclopentadienyl(triphenylphosphine)-gold(I) ($\text{Ph}_4\text{HC}_5\text{AuPPh}_3$). *J. Organomet. Chem.* **1981**, *220*, 125–137. (c) Perevalova, E. G.; Grandberg, K. J.; Dyadchenko, V. P.; Baukova, T. V. New organogold complexes: tetraphenylcyclopentadiene derivatives. *J. Organomet. Chem.* **1981**, *217*, 403–413. (d) Halim, M.; Kennedy, R. D.; Suzuki, M.; Khan, S. I.; Diaconescu, P. L.; Rubin, Y. Complexes of Gold(I), Silver(I), and Copper(I) with Pentaaryl[60]fullerides. *J. Am. Chem. Soc.* **2011**, *133*, 6841–6851. (e) Werner, H.; Otto, H.; Ngo-Khac, T.; Burschka, C. Synthese und eigenschaften neuer kupfer-und gold-komplexe des typs $\text{C}_5\text{H}_5\text{MPR}_3$, $\text{C}_5\text{Me}_5\text{MPR}_3$, und $\text{R}'\text{C}_2\text{MPR}_3$ ($\text{M} = \text{Cu}, \text{Au}$) sowie die kristallstruktur von $\text{C}_5\text{H}_5\text{AuPPr}_3$. *J. Organomet. Chem.* **1984**, *262*, 123–136. (f) Schumann, H.; Gorlitz, F. H.; Dietrich, A. Pentabenzylcyclopentadienyl(triphenylphosphine)gold(I). *Chem. Ber.* **1989**, *122*, 1423–1426. (g) Bruce, M. I.; Walton, J. K.; Skelton, B. W.; White, A. H. Pentakis(methoxycarbonyl)cyclopentadiene chemistry. Part 5. Preparation and crystal and molecular structures of $[\text{Au}\{\text{C}_5(\text{CO}_2\text{Me})_5\}(\text{PPh}_3)]$ and $[\text{Au}(\text{PPh}_3)_2[\text{C}_5(\text{CO}_2\text{Me})_5]\bullet\text{MeOH}$. *J. Chem. Soc., Dalton Trans.* **1983**, 809–814.

(25) (a) Campbell, C. H.; Green, M. L. H. Studies on the temperature dependence in the ^1H NMR spectra of some methylcyclopentadienyl metal compounds. *J. Chem. Soc. A* **1971**, 3282–3285. (b) Ortaggi, G. An infrared and NMR study of the structure of cyclopentadienyl compounds of gold(I). *J. Organomet. Chem.* **1974**, *80*, 375–279. (c) Hüttel, R.; Raffay, U.; Reinheimer, H. Cyclopentadienylgold(I) and Cyclopentadienyl(triphenylphosphine)gold(I). *Angew. Chem. Int. Ed.* **1967**, *6*, 862. (d) Smyslova, E. I.; Perevalova, E. G.; Dyadchenko, V. P.; Grandberg, K. J.; Slovokhotov, Y. L.; Struchkov, Y. T. Syntheses OF Organogold(1+) Compounds by Direct Auration. *J. Organomet. Chem.* **1981**, *215*, 269–279.

(26) Sapsford, K. E.; Algar, W. R.; Berti, L.; Gemmill, K. B.; Casey, B. J.; Oh, E.; Stewart, M. H.; Medintz, I. L. Functionalizing Nanoparticles with Biological Molecules: Developing Chemistries that Facilitate Nanotechnology. *Chem. Rev.* **2013**, *113*, 1904–2074.

(27) (a) Stradiotto, M.; Hughes, D. W.; Bain, A. D.; Brook, M. A.; McGlinchey, M. J. The Fluxional Character of $(\eta^5\text{C}_5\text{H}_5)\text{Fe}(\text{CO})_2(\eta^1\text{C}_9\text{H}_7)$: Evidence for the [4 + 2] cycloaddition of a metal-substituted isoindene with tetracyanoethylene. *Organometallics* **1997**, *16*, 5563–5568. (b) Casey, C. P.; O'Connor, J. M. The η^5 to η^1 conversions of indenyltricarbonylrhenium. *Organometallics* **1985**, *4*, 384–388. (c) Saegusa, T.; Ito, Y.; Tomita, S. Cyclopentadienylcopper(I)-isocyanide complex. New preparative method and catalyst activity. *J. Am. Chem. Soc.* **1971**, *93*, 5656–5661. (d) Stradiotto, M.; McGlinchey, M. J. η^1 -Indenyl derivatives of transition metal and main group elements: synthesis, characterization, and molecular dynamics. *Coord. Chem. Rev.* **2001**, *219–221*, 311–378. (e) Kitching, W.; Hegarty, B. F. Concerning the structures of cyclopentadienyl mercurials. *J. Organomet. Chem.* **1969**, *16*, 39–44. (f) Kitching, W. Hegarty, B. F.; Doddrell, D. Structural studies of indenylmercury systems. *J. Organomet. Chem.* **1970**, *21*, 29–36. (g) Cotton, F. A.; Hunter, D. L.; Jamerson, J. D. A carbon-13 NMR study of the rearrangement pathway of the fluxional molecule cyclopentadienylmercury chloride and some related compounds. *Inorg. Chim. Acta* **1975**, *15*, 245–247. (h) Bellomo, S.; Ceccon, A.; Gambaro, A.; Santi, S. A stable dicarbonyl(cycloocta-1,5-diene)- $(\eta^1\text{-indenyl})$ iridium intermediate in the substitution reaction of cycloocta-1,5-diene($\eta^5\text{-indenyl}$)iridium with carbon monoxide. *J. Organomet. Chem.* **1993**, *453*, C4–C6. (i) Cecchetto, P.; Ceccon, A.; Gambaro, A.; Santi, S.; Ganis, P.; Gobetto, R.; Valle, G.; Venzo, G. Heterobimetallic Indenyl Complexes. Synthesis and Carbonylation Reaction of anti-[$\text{Cr}(\text{CO})_3\mu,\eta^1\text{-indenyl}-\text{Ir}(\text{COD})$]. *Organometallics* **1998**, *17*, 752–762. (j) Cotton, F. A.; Musco, A.; Yagupsky, G. Stereochemically nonrigid organometallic molecules. VIII. Further studies of σ -cyclopentadienylmetal compounds. *J. Am. Chem. Soc.* **1967**, *89*, 6136–6139.

(28) (a) Bates, G. S.; Ramaswamy, S. A Thermal [1,3] Sigmatropic Rearrangement Thermolysis of 2,2-bis(ethylthio)-3,3-dimethyl-4-pentenyl. *Can. J. Chem.* **1981**, *59*, 3120–3122. (b) Spangler, C. W. Thermal [1,j] sigmatropic rearrangements. *Chem. Rev.* **1976**, *76*, 187–217.

(29) Grandberg, K. I.; Dyadchenko, V. P. Some aspects of the organometallic chemistry of univalent gold. *J. Organomet. Chem.* **1994**, *474*, 1–21.

(30) (a) Brown, T. J.; Dickens, M. G.; Widenhoefer, R. A. Syntheses and X-ray crystal structures of cationic, two-coordinate gold(I) π -alkene complexes that contain a sterically hindered o-biphenylphosphine ligand. *Chem. Commun.* **2009**, 6451–6453. (b) Brown, T. J.; Dickens, M. G.; Widenhoefer, R. A. Syntheses, X-ray Crystal Structures, and Solution Behavior of Monomeric, Cationic, Two-Coordinate Gold(I) π -Alkene Complexes. *J. Am. Chem. Soc.* **2009**, *131*, 6350–6351.

(31) (a) Espada, M. F.; Campos, J.; López-Serrano, J.; Poveda, M. L.; Carmona, E. Methyl-, Ethenyl-, and Ethynyl-Bridged Cationic Di-gold Complexes Stabilized by Coordination to a Bulky Terphenylphosphine Ligand. *Angew. Chem., Int. Ed.* **2015**, *54*, 15379–15384. (b) Miranda-Pizarro, J.; Luo, Z.; Moreno, J. J.; Dickie, D. A.; Campos, J.; Gunnoe, T. B. Reductive C–C Coupling from Molecular Au(I) Hydrocarbyl Complexes: A Mechanistic Study. *J. Am. Chem. Soc.* **2021**, *143*, 2509–2522.

(32) Burdett, J. K.; Eisenstein, O.; Schweizer, W. B. Are Strong Gold–Gold Interactions Possible in Main Group $\text{X}_n\text{A}(\text{AuPR}_3)_m$ Molecules? *Inorg. Chem.* **1994**, *33*, 3261–3268.

(33) Brooner, R. E. M.; Widenhoefer, R. A. Syntheses, X-ray Crystal Structures, and Solution Behavior of Cationic, Two Coordinate Gold(I) η^2 -Diene Complexes. *Organometallics* **2011**, *30*, 3182–3193.

(34) Sanguramath, R. S.; Patra, S. K.; Green, M.; Russell, C. A. The coordination and polymerisation of cyclic 1,3-dienes by gold(I) cations. *Chem. Commun.* **2012**, *48*, 1060–1062.

(35) *Gaussian 16, Revision A.03*, Frisch, M. J.; Trucks, G. W.; Schlegel, H. B.; Scuseria, G. E.; Robb, M. A.; Cheeseman, J. R.; Scalmani, G.; Barone, V.; Petersson, G. A.; Nakatsuji, H.; Li, X.; Caricato, M.; Marenich, A. V.; Bloino, J.; Janesko, B. G.; Gomperts, R.; Mennucci, B.; Hratchian, H. P.; Ortiz, J. V.; Izmaylov, A. F.; Sonnenberg, J. L.; Williams-Young, D.; Ding, F.; Lipparini, F.; Egidi, F.; Goings, J.; Peng, B.; Petrone, A.; Henderson, T.; Ranasinghe, D.; Zakrzewski, V. G.; Gao, J.; Rega, N.; Zheng, G.; Liang, W.; Hada, M.; Ehara, M.; Toyota, K.; Fukuda, R.; Hasegawa, J.; Ishida, M.; Nakajima, T.; Honda, Y.; Kitao, O.; Nakai, H.; Vreven, T.; Throssell, K.; Montgomery, J. A., Jr.; Peralta, J. E.; Ogliaro, F.; Bearpark, M. J.; Heyd, J. J.; Brothers, E. N.; Kudin, K. N.; Staroverov, V. N.; Keith, T. A.; Kobayashi, R.; Normand, J.; Raghavachari, K.; Rendell, A. P.; Burant, J. C.; Iyengar, S. S.; Tomasi, J.; Cossi, M.; Millam, J. M.; Klene, M.; Adamo, C.; Cammi, R.; Ochterski, J. W.; Martin, R. L.; Morokuma, K.; Farkas, O.; Foresman, J. B.; Fox, D. J. *Gaussian, Inc.*, Wallingford CT, 2016.

(36) (a) Becke, A. D. Density-functional thermochemistry. III. The role of exact exchange. *J. Chem. Phys.* **1993**, *98*, 5648–5652. (b) Lee, C.; Yang, W.; Parr, R. G. Development of the Colle-Salvetti correlation-

energy formula into a functional of the electron density. *Phys. Rev. B* **1988**, *37*, 785–789.

TOC graphic

